Available online at www.sciencedirect.com
ScienceDirect
Journal of Power Sources 163 (2006) 278–283
JOURNAL OF POWER SOURCES
www.elsevier.com/locate/jpowsour

Short communication

Preparation of $LiMn_2O_4$ at the low temperature of 250 °C using eutectic self-mixing method

Ji-Woo Na, Ja-Young Kwon, Kyoo-Seung Han *

Department of Fine Chemical Engineering and Chemistry, Chungnam National University, Daeduk Science Town, Taejeon 305-764, South Korea

Received 22 August 2005; received in revised form 16 May 2006; accepted 27 May 2006
Available online 24 July 2006

Abstract

Spinel $LiMn_2O_4$ as a cathode material for lithium rechargeable batteries is prepared at the low temperature of 250 °C without any artificial mixing procedures of reactants. The phase transitions of lithium manganese oxide are found three times on heating at 250 °C. The prepared material exhibits the initial discharge capacity of 85.5 mAh g^{-1} and the discharge capacity retention of 91.5% after 50 cycles.
© 2006 Elsevier B.V. All rights reserved.

Keywords: Eutectic self-mixing method; $LiMn_2O_4$; Lithium rechargeable battery; Cathode

1. Introduction

Lithium manganese oxides have been studied extensively as cathode materials for lithium rechargeable batteries [1–13]. These lithium manganese oxides could be bisected by their synthetic temperature: (1) spinel phase $LiMn_2O_4$ prepared over 700 °C (HT-$LiMn_2O_4$) and (2) "low-temperature $LiMn_2O_4$" (LT-$LiMn_2O_4$) prepared around 450 °C. It is found that those electrochemical properties depend on the synthetic temperature. While spinel $LiMn_2O_4$ shows two potential plateaus in the 4 V range and a potential plateau in the 3 V range, LT-$LiMn_2O_4$ exhibits just two plateaus in the 3 V range without potential plateau in the 4 V range [6,7]. It has been considered that the different potential plateaus in the 4 V range and the 3 V range for $LiMn_2O_4$ correspond to the intercalations of lithium into the 8a tetrahedral sites and the 16c octahedral sites, respectively. Nevertheless, in this regard, no apparent potential plateau in the 4 V range for LT-$LiMn_2O_4$ chaotically represents that LT-$LiMn_2O_4$ is not crystallized in spinel structure.

Here, we present that spinel phase $LiMn_2O_4$ can be prepared at 250 °C using the eutectic self-mixing method.

2. Experimental

2.1. Materials

Both 0.1 mol of $LiCH_3CO_2{\cdot}2H_2O$ (98%, Aldrich Co., USA) and 0.2 mol of $Mn(CH_3CO_2)_2{\cdot}4H_2O$ (>99%, Aldrich Co., USA) were consecutively heated up to their eutectic temperature (70 °C) for 40 min and 250 °C for 24 h in air without any artificial mixing and intermittent cooling procedures. Independently, other lithium manganese oxides were prepared to investigate the phase changes on the preparation of $LiMn_2O_4$ at 250 °C using the eutectic self-mixing method. The synthetic conditions and the designations on samples are listed in Table 1.

2.2. Characterization

Thermal analysis of the acetates was performed at a rate of >1 °C min^{-1}, from room temperature to 1000 °C, in air using SDT 2960 TG-DTA (TA Instruments). ^{7}Li NMR measurements were carried out at room temperature on Bruker DSX 400 with a 9.4 T magnet. Magic angle spinning (MAS) NMR experiments were performed using a 4 mm CP-MAS probe and zirconia sample rotor. The ^{7}Li resonance frequency used was 155.6 MHz; a sample spinning speed of 14 kHz was employed. Spectra were acquired using single-pulse and echo-pulse sequences. Both quadrupolar echoes and spin-echoes were used to acquire spectra of all samples. However, the spectra were subsequently acquired

* Corresponding author. Tel.: +82 42 821 5897; fax: +82 42 822 6637.
E-mail address: kshan@cnu.ac.kr (K.-S. Han).

0378-7753/$ – see front matter © 2006 Elsevier B.V. All rights reserved.
doi:10.1016/j.jpowsour.2006.05.047

Table 1
Heating temperatures and reaction times to prepare the samples as well as their designations

Label	Heating temperature and reaction time
M1	70 °C, 10 min
M2	70 °C, 40 min
M3	70 °C, 40 min + 250 °C, 10 min
M4	70 °C, 40 min + 250 °C, 2 h
M5	70 °C, 40 min + 250 °C, 8 h
M6	70 °C, 40 min + 250 °C, 12 h
M7	70 °C, 40 min + 250 °C, 24 h
M8	70 °C, 40 min + 250 °C, 48 h
M9	70 °C, 40 min + 250 °C, 72 h
M10	70 °C, 40 min + 250 °C, 96 h

The reactants are $LiCH_3CO_2{\cdot}2H_2O$ and $Mn(CH_3CO_2)_2{\cdot}4H_2O$.

with echo-pulse sequences to ensure that no resonances were missed with single-pulse sequence. All spectra were referenced to an external 1 M LiCl solution; a 90° pulse-length of 4.3 μs, repetition delay of 0.1 s, and spectral width of 0.7 MHz were used. For enhancement of spectral resolution, 256–20,000 acquisitions were used. Elemental analysis of the prepared phases was carried out by ICP-AES (Jobin Yvon, JY38S) and Carlo Erba EA 1108 CHN analyzer. X-ray diffraction (XRD) pattern analyses were achieved by using a Mac Science M03XHF[22] diffractometer and Cu Kα radiation ($\lambda = 1.5405$ Å) operated with 30 mA and 40 kV. The diffractograms were recorded in the 2θ range of 5–90° with 0.02° intervals at a scanning rate of 2° min^{-1}. Mn K-edge X-ray absorption spectroscopy (XAS) data were obtained using the BL7C1 beam-line of Pohang Light Sources (PLS). Synchrotron radiation from the electron storage ring (2.5 GeV with about 120–170 mA of stored current) was monochromatized with a Si(3 1 1) double-crystal monochromator. All Mn K-edge XAS data were collected in transmission mode at room temperature. Absorbance was measured with the ionization chamber filled with N_2(85%) + Ar(15%) and N_2(100%) for incident and transmitted beams, respectively. The high order harmonics have been eliminated with detuning to 70% of incident beam intensity. The monochromatic X-ray beam has been used with the energy resolution ($\Delta E/E$) below 2×10^{-4}. The energy of each spectrum was calibrated from the energy scale of the Mn metal spectra. To remove the energy shift problem, the X-ray absorption spectrum for the metal foil has been measured simultaneously in every measurement as the metal foil was positioned in front of the window of the third ion chamber. The absorbance $\mu(E)$ was normalized to an edge-jump of unity to compare the X-ray absorption near-edge structure (XANES) features directly with one another. The EXAFS data analyses have been carried out by the standard procedure elsewhere. The measured absorption spectrum below the pre-edge region was fitted to a straight line, and then the background contribution above the post-edge region, $\mu_o(E)$, was fitted to a high order polynomial. The fitted polynomials have been extrapolated through the total energy region and subtracted from the total absorption spectra. The background-subtracted absorption spectra were normalized for the above energy region, $\chi(E) = \{\mu(E) - \mu_o(E)\}/\mu_o(E)$. The normalized k^3-weighted EXAFS spectra, $k^3\chi(k)$, have been Fourier transformed in the k range from 2.0 to 14.0 $Å^{-1}$ with the hanning window function in order to show the contribution of each bond pair on the Fourier transform (FT) peak. The presence of lithium and the valency of the manganese in the prepared phases were cross-checked using X-ray photoelectron spectrometry (XPS; ESCA3200, Shimadzu) with Mg Kα radiation. Electrochemical tests were carried out at room temperature using coin cells. The prepared cathode materials were mixed with 9 wt.% super-P carbon black and 8 wt.% poly-vinylidene fluoride (PVDF) binder dissolved in *N*-methyl-2-pyrrolidone (NMP) until a slurry was obtained. The slurry was laminated on an Al foil using a hot-roller press. The electrolyte was a 1.0 M solution of $LiPF_6$ in ethylene carbonate (EC) and ethyl methyl carbonate (EMC) with 1:2 volume ratio. Lithium foil was used as anode; cell assembly was performed in an Ar-filled glove box; cells were charged and discharged at C/5.

3. Results and discussion

The TG-DTA curves in Fig. 1 ascertain that the first weight loss (29.8%) between room temperature and 170 °C together with small endothermic DTA peaks around 100 °C correspond to the removal of hydrated $10H_2O$ (30.4%). Beyond 170 °C up to 250 °C, decomposition of lithium acetate and manganese acetate results in the second weight loss of 38.8% and two large exothermic DTA peaks around 250 °C. This result agrees well with the calculated value, 39.0% for the release of $7.5H_2O$ and $10CO_2$, as well as the gain of $10.75O_2$. The decomposition of both acetates around 250 °C releases mass heat. This exothermic heat is predicted to be utilized as the lattice energy required for the formation of $LiMn_2O_4$ phase. As shown in Fig. 1, the temperature of 250 °C is the end-point for all of thermal weight loss, endothermic and exothermic, which means it is possible to prepare $LiMn_2O_4$ phase at a low temperature around 250 °C.

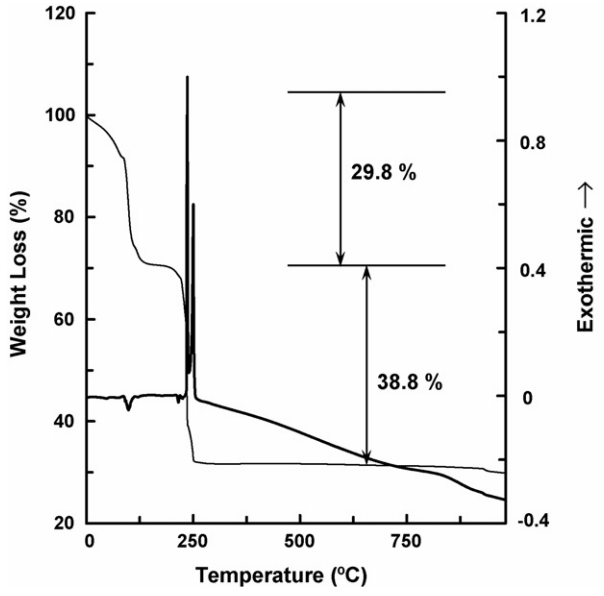

Fig. 1. TG-DTA curves of $LiCH_3CO_2{\cdot}2H_2O$ and $Mn(CH_3CO_2)_2{\cdot}4H_2O$ measured at a heating rate of 1 °C min^{-1} under an oxygen flow.

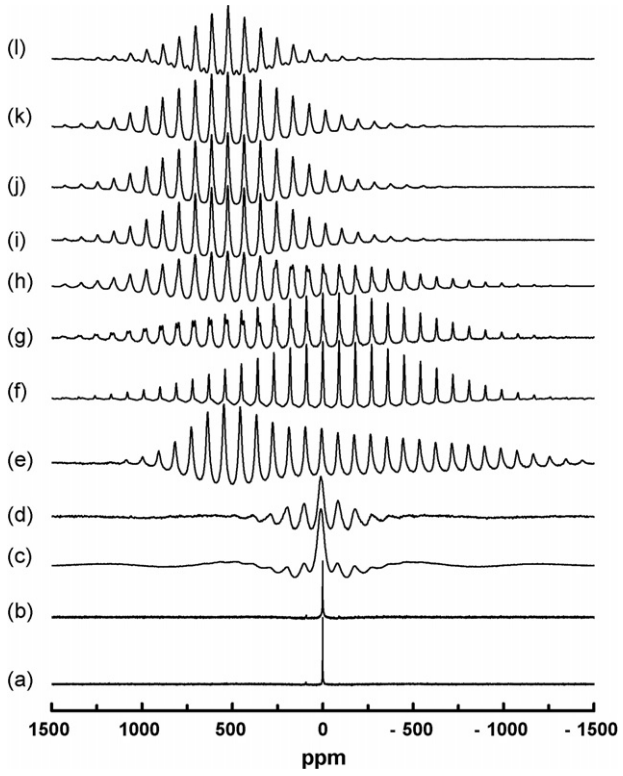

Fig. 2. ^{7}Li MAS NMR spectra of: (a) $LiCH_3CO_2{\cdot}2H_2O$, (b) lithium acetate heated at 70 °C for 40 min, (c) M1, (d) M2, (e) M3, (f) M4, (g) M5, (h) M6, (i) M7, (j) M8, (k) M10, and (l) reference $LiMn_2O_4$ phase. All spectra were acquired at room temperature with spinning speeds of 14 kHz.

The reaction pathway can thus be given as follows:

$$LiCH_3CO_2{\cdot}2H_2O + 2Mn(CH_3CO_2)_2{\cdot}4H_2O \rightarrow LiMn_2(CH_3CO_2)_5 + 10H_2O \quad (1)$$

$$LiMn_2(CH_3CO_2)_5 + 10.75O_2 \rightarrow LiMn_2O_4 + 7.5H_2O + 10CO_2 \quad (2)$$

To elucidate the possible preparation of $LiMn_2O_4$ phase at 250 °C, the prepared materials were subsequently analyzed with respect to its structure and battery performances.

The ^{7}Li MAS NMR spectroscopy has been used to study the changes in the local environments of lithium during the preparation of $LiMn_2O_4$ at 250 °C using the eutectic self-mixing method. Fig. 2 shows the ^{7}Li MAS NMR spectra of thermally exposed reactants at various conditions. The spectrum of $LiCH_3CO_2{\cdot}2H_2O$ shows a sharp resonance having very weak spinning sidebands with an isotropic resonance at ~0 ppm. This is a typical spectrum of a normal diamagnetic solid solution. As shown in Fig. 2(b), the chemical environment of lithium in lithium acetate alone heated at 70 °C for 40 min remains unchanged. Separately, in case of lithium acetate and manganese acetate heated at 70 °C, the NMR spectra of M1 and M2 show significantly broadened isotropic line with the trivial chemical shift and the enhanced spinning sideband manifolds compared to those of $LiCH_3CO_2{\cdot}2H_2O$ and lithium acetate alone heated at 70 °C for 40 min. The enhancement of spinning sideband manifolds is caused by the increased portion of paramagnetic manganese around lithium, and the spectral line broadening is originated from the anisotropic bulk magnetic susceptibility [14,15]. These critical features indicate that the molten acetates in this synthetic procedure are mixed by themselves.

Three characteristic features can be seen in the NMR spectra of M3; the abrupt isotropic shift moving to lower field, the markedly enhanced spinning sideband manifolds, and the drastically broadened spectral width. The Fermi contact shift by the interaction between the unpaired electron spins of manganese and nuclear spins of lithium causes the abrupt isotropic chemical shift [16,17]. Thus, this dominant resonance can be assigned to the lithium, existed as an intermediate, in a lithium manganese oxide.

As shown in Fig. 2(f and g), another isotropic resonance at ~0 ppm is detected. In ^{7}Li NMR, a resonance at ~0 ppm is usually observed for a diamagnetic solid solution, such as lithium acetate. For the conditions of our experiment, this signal is expected due to rather decomposition of lithium acetate than diamagnetic solid solution. To verify the chemical environment of lithium in M4 and M5 having this unusual chemical shift, elemental analysis of these samples was performed. In M4 and M5, the wt.% of carbon was determined below system error, which indicates that lithium acetate or possible impurities such as lithium carbonate are not present. Furthermore, it was found by iodometric titration that the average oxidation state of manganese in both M4 and M5 is higher than that of spinel $LiMn_2O_4$ containing both Mn^{4+} and Mn^{3+} ions in a 1:1 ratio. Since the chemical shift of the ^{7}Li resonance for lithium manganate having Mn^{4+} is varying by the combination of semi-linear and bent (90°) Li–O–Mn bonds, it would be shifted to ~0 ppm [17]. Therefore, the dominant resonance for M4 can be assigned to the lithium in the second intermediate. Also, a resonance at 523 ppm is observed in Fig. 2(g and h), which can be certainly assigned to lithium in the general position, 8a, of spinel $LiMn_2O_4$ structure by the Fermi contact shift mechanism as expected [17]. Therefore, all the lithium atoms under this condition are interacted with manganese, which directly indicates a successful homogeneous mixing of reactants through the eutectic self-mixing procedure as well as the possible preparation of $LiMn_2O_4$ phase at 250 °C. M7, M8, and M10 exhibit a single resonance at 523 ppm, which shows the complete phase transition from the second intermediate to spinel $LiMn_2O_4$ with the increase of reaction time. Therefore, the phase transitions of lithium manganese oxide are obviously found three times on the heating at 250 °C for 24 h.

By the way, the spectrum of reference $LiMn_2O_4$ contains the resonance at 523 ppm and an additional resonance weakly at 566 ppm, as shown in Fig. 2(l). The later is generally originated from the inevitable crystalline imperfections such as vacancies on both the lithium and manganese sites. These are consistent with the results previously reported by Morgan et al. and Lee et al. [16,17].

The $LiMn_2O_4$ phases prepared at 250 °C using eutectic self-mixing method and the reference $LiMn_2O_4$ phase were characterized with respect to those macro and micro structures by

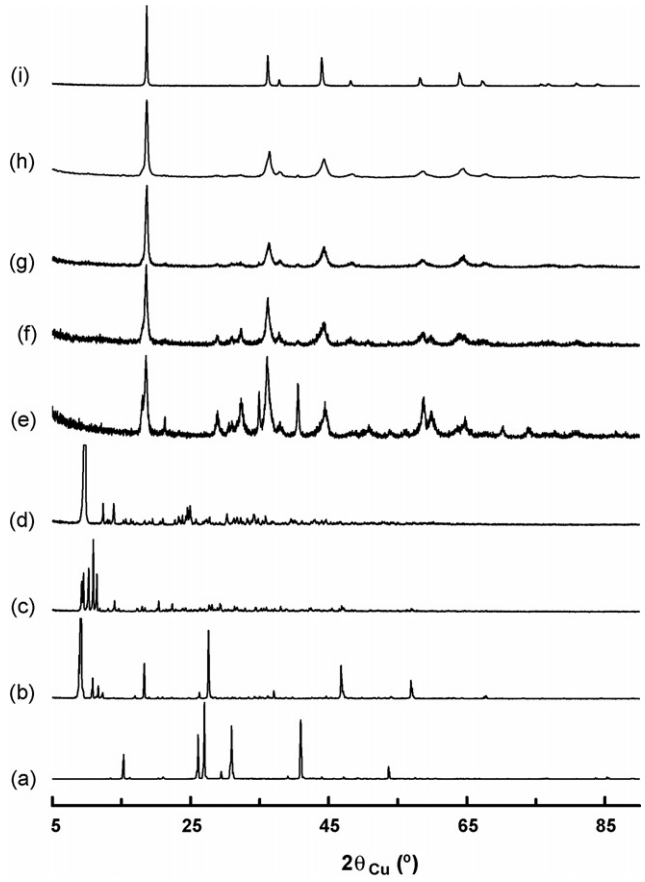

Fig. 3. X-ray diffraction patterns of: (a) $LiCH_3CO_2{\cdot}2H_2O$, (b) $Mn(CH_3CO_2)_2{\cdot}4H_2O$, (c) M2, (d) M3, (e) M4, (f) M5, (g) M7, (h) M10, and (i) reference $LiMn_2O_4$ phase.

the XRD pattern analysis and the XAS analysis, respectively. The XRD patterns are shown in Fig. 3. Although the reference $LiMn_2O_4$ exhibits all XRD peaks characteristic for the space group *Fd*3*m* as spinel $LiMn_2O_4$ phase, the $LiMn_2O_4$ phases prepared at 250 °C for 24 and 96 h using eutectic self-mixing method is supposed to have a spinel structure mixed with ramsdellite structure (space group *Pnam*). Mn K-edge XAS spectra of the $LiMn_2O_4$ phases prepared at 250 °C using eutectic self-mixing method and the reference $LiMn_2O_4$ phase are shown in Figs. 4 and 5. Mn K-edge XANES spectra in Fig. 4 shows the evolution of the oxidation state of the central Mn atom, the bond covalency, and the local structure around the Mn atom during the preparation of $LiMn_2O_4$ at 250 °C. Separately, variations in Fourier transform magnitude of Mn K-edge EXAFS spectra in Fig. 5 shows the increase of the structural regularity with the increased heating time at 250 °C. The FT magnitude at ∼1.5 Å corresponds to six-coordinated oxygen of the nearest neighboring atom around the Mn atom, while the other FT magnitude at ∼2.5 Å is assigned to the contribution of six Mn atoms as a second neighboring atom. As the results of EXAFS curve fitting for the $LiMn_2O_4$ phases prepared at 250 °C for 24 and 96 h as well as the reference $LiMn_2O_4$ phase, the bond distances of Mn–O and Mn–Mn remain constant as 1.93 and 2.93 Å, respectively, irrespective of the synthetic temperature. The similar appearances of the Mn K-edge XAS spectra of the $LiMn_2O_4$ phases prepared

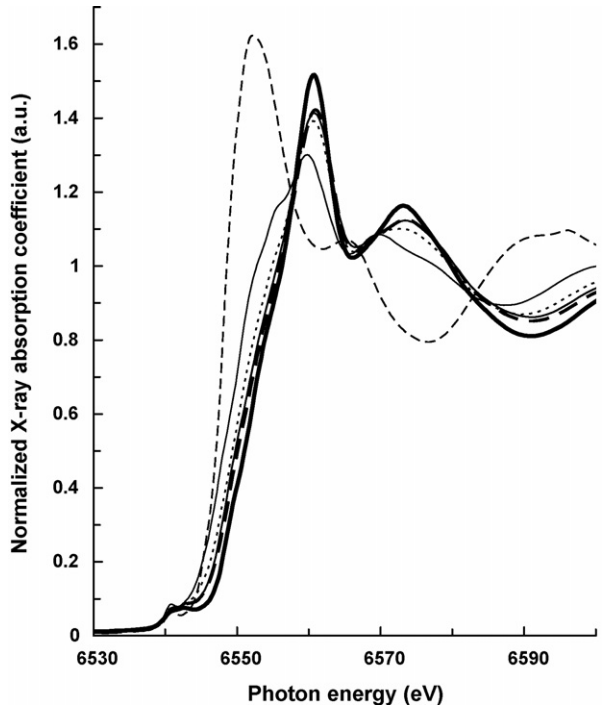

Fig. 4. Mn K-edge XANES spectra of M3 (- - -), M5 (—), M6 (· · ·), M7 (▬▬), M10 (▬ ▬ ▬), and reference $LiMn_2O_4$ phase (▬).

at 250 °C for 24 and 96 h using eutectic self-mixing method and the reference $LiMn_2O_4$ phase suggest that the Mn atoms in three $LiMn_2O_4$ phases are in the similar physicochemical state.

Figs. 6 and 7 show the Li 1s plus Mn 3p, and Mn $2p_{3/2}$ plus Mn $2p_{1/2}$ XPS spectra, respectively, of the reference $LiMn_2O_4$

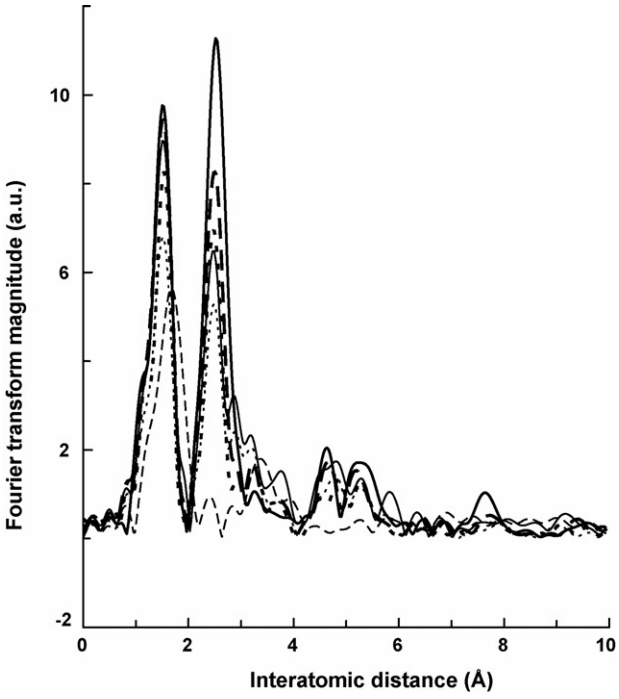

Fig. 5. Variations in Fourier transform magnitude of Mn K-edge EXAFS spectra for M3 (- - -), M5 (· · ·), M6 (.....), M7 (▬▬), M10 (▬ ▬ ▬), and reference $LiMn_2O_4$ phase (▬).

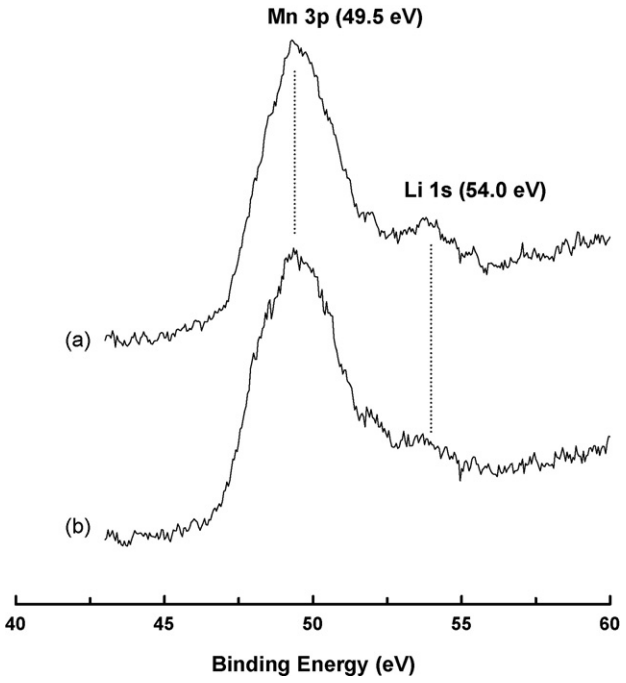

Fig. 6. Li 1s XPS and Mn 3p XPS data for: (a) the reference $LiMn_2O_4$ phase and (b) M10.

phase and M10. In Fig. 6, although the protruding part around 54 eV of the Mn 3p XPS band might be analogized to Li 1s XPS band, a detailed analysis of the presence of lithium in M10 using XPS is prevented by the foreseen superposition of Li 1s and Mn 3p XPS bands. However, the presence of lithium in M10 can be indirectly confirmed by the oxidation state of manganese in M10. In Fig. 7, the Mn 2p XPS spectrum consists of a Mn $2p_{3/2}$ XPS core line at 642.2 eV and a Mn $2p_{1/2}$ XPS line at 653.7 eV

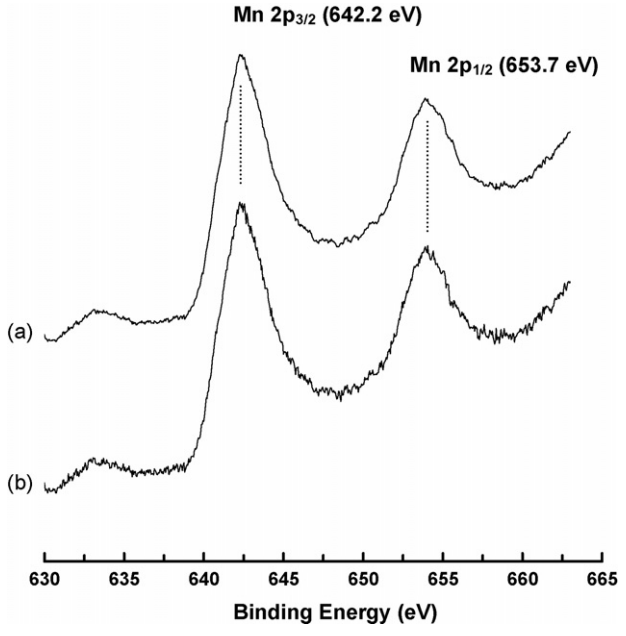

Fig. 7. Mn 2p XPS data for: (a) the reference $LiMn_2O_4$ phase and (b) M10.

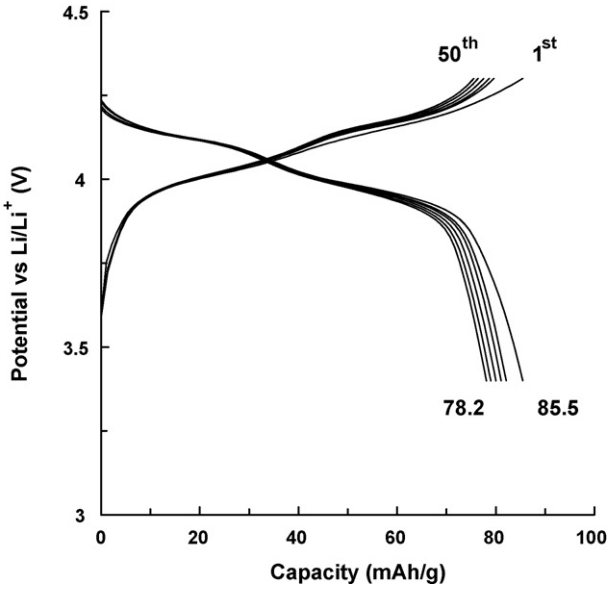

Fig. 8. Voltage vs. capacity profiles for the $LiMn_2O_4$ phase prepared at 250 °C for 24 h using the eutectic self-mixing method.

as an 11.5 eV higher binding energy. Considering the Mn $2p_{3/2}$ XPS core lines of Mn_2O_3 at 641.6 eV and MnO_2 at 642.6 eV, the Mn $2p_{3/2}$ XPS core line of M10 at 642.2 eV indicates the intermediate valency of the manganese in M10 between trivalent and tetravalent. The presence of trivalent manganese in M10 directly means the presence of lithium in M10. Thus, a mixed valence Mn^{3+}/Mn^{4+} in M10 may suggest the possible preparation of spinel phase $LiMn_2O_4$ at 250 °C using the eutectic self-mixing method.

As shown in Fig. 8, the $LiMn_2O_4$ phase prepared at 250 °C for 24 h using eutectic self-mixing method exhibits the initial discharge capacity of 85.5 mAh g^{-1} in the voltage range of 3.4–4.3 V and the discharge capacity retention of 91.5% after 50 cycles. Although the discharge capacity of the $LiMn_2O_4$ phase prepared at 250 °C for 24 h is poor in comparison with that of the spinel phase $LiMn_2O_4$ prepared over 700 °C (∼125 mAh g^{-1}), its initial open-circuit voltage of 3.41 V and two potential plateaus in the 4 V range are the typical properties for spinel phase $LiMn_2O_4$. These results represent the successful preparation of $LiMn_2O_4$ at 250 °C using the eutectic self-mixing method.

4. Conclusion

Spinel $LiMn_2O_4$ as a cathode material for lithium rechargeable batteries is prepared at a low temperature of 250 °C using the eutectic self-mixing method without any artificial mixing procedure. The spontaneous and homogeneous mixes as well as several phase transitions during the preparation of spinel $LiMn_2O_4$ at 250 °C are demonstrated by ^7Li MAS NMR spectroscopy. The prepared material exhibits the initial discharge capacity of 85.5 mAh g^{-1} and the discharge capacity retention of 91.5% after 50 cycles.

Acknowledgement

This work was funded by Korea Research Foundation Grant (KRF-12005-005-J00403) and BK21-E2M.

References

[1] Y. Gao, J.R. Dahn, J. Electrochem. Soc. 143 (1996) 100.
[2] C. Masquelier, M. Tabuchi, K. Ado, R. Kanno, Y. Kobayashi, Y. Maki, O. Nakamura, J.B. Goodenough, J. Solid State Chem. 123 (1996) 255.
[3] S. Choi, A. Manthiram, J. Electrochem. Soc. 147 (2000) 1623.
[4] J.P. Cho, M.M. Thackeray, J. Electrochem. Soc. 146 (1999) 3577.
[5] J.M. Tarascon, D. Guyomard, Electrochim. Acta 38 (1993) 1221.
[6] S.H. Kang, J.B. Goodenough, J. Electrochem. Soc. 147 (2000) 3621.
[7] Y. Nitta, K. Okamura, M. Nagayama, A. Ohta, J. Power Sources 68 (1997) 166.
[8] S.R.S. Prabaharan, N.B. Saparil, S.S. Michael, M. Massot, C. Julien, Solid State Ionics 112 (1998) 25.
[9] T. Takada, H. Hayakawa, E. Akiba, F. Izumi, B.C. Chakoumakos, J. Power Sources 68 (1997) 613.
[10] J. Kim, A. Manthiram, J. Electrochem. Soc. 145 (1998) L53.
[11] M.M. Thackeray, A. de Koch, M.H. Rossouw, D. Liles, R. Bittihn, D. Hoge, J. Electrochem. Soc. 139 (1992) 363.
[12] T. Le Mercier, J. Gaubicher, E. Bermejo, Y. Chabre, M. Quarton, J. Mater. Chem. 9 (1999) 567.
[13] P. Mustarelli, V. Massarotti, M. Bini, D. Capsoni, Phys. Rev. B 55 (1997) 12018.
[14] W.P. Rothwell, J.S. Waugh, J.P. Yesinowski, J. Am. Chem. Soc. 102 (1980) 2637.
[15] A. Nayeem, J.P. Yesinowski, J. Chem. Phys. 89 (1988) 4600.
[16] K.R. Morgan, S. Collier, G. Burns, K. Ooi, J. Chem. Soc. Chem. Commun. 2 (1994) 1719.
[17] Y.J. Lee, F. Wang, C.P. Grey, J. Am. Chem. Soc. 120 (1998) 12601.